GSA Data Repository item 2011339

Appendix DR1. Microscopy and microanalysis, SHRIMP analytical procedures and data interpretation, Figures DR1–DR5 and Tables DR1–DR11

Metamorphic replacement of mineral inclusions in detrital zircon from Jack Hills: Implications for the Hadean Earth

by Birger Rasmussen, Ian R. Fletcher, Janet R. Muhling, Courtney J. Gregory, Simon A. Wilde

MICROSCOPY AND MICROANALYSIS

Imaging and analysis of inclusions

Five epoxy mounts of detrital zircon from Jack Hills were cleaned and coated with a carbon film. Zircons were imaged with a JEOL 6400 SEM using secondary electron (SE), back-scattered electron (BSE) and cathodoluminscence (CL) modes. Each inclusion was analyzed using energy dispersive X-ray spectrometry (EDS), which provided qualitative data to determine the mineral chemistry (see Table DR1).

Zircon grain separates from twenty-five samples of Precambrian igneous rocks from Western Australia were also examined by SEM-EDS to investigate the inclusion assemblage of possible source rocks for the Jack Hills zircons (Fig. DR1; Tables DR2 and DR3). The sample identification numbers given below are from the Geological Survey of Western Australia (GSWA): 169044A & B (muscovite-biotite monzogranite); 178078 (biotite monzogranite); 178049 (biotite monzogranite); 142937 (leucocratic monzogranite); 184811 (biotite monzogranite); 169096 (monzogranite); 169097 (monzogranite); 179435 (biotite monzogranite); 178101 (biotite monzogranite); 178425 (biotite monzogranite); 178103 (biotite monzogranite); 139464 (biotite monzogranite); 169055 (biotite-muscovite monzogranite); 169018 (biotite monzogranite); 169062 (syenogranite); 169028 (granodiorite); 177933 (hornblende granodiorite); 177932 (foliated granodiorite); 178104 (biotite granodiorite); 139466 (granodiorite); 160212 (biotite-hornblende tonalite); 178002 (biotite tonalite); 178077 (biotite tonalite); 178102 (hornblende tonalite).

Muscovite analysis

Muscovite analyses (Figs. DR2, 3; Tables DR4-6) were collected with an Oxford Instruments Link Analytical Si(Li) Energy Dispersive Spectrometer attached to a JEOL 6400 SEM at 15 kV accelerating voltage and 5 nA beam current. The instrument was calibrated for quantitative analysis using albite (Na), periclase (Mg), corundum (Al), wollastonite (Si, Ca), NaCl (Cl), orthoclase (K), rutile (Ti) and pure metals (Cr, Mn, Fe, Ni) as standards. Repeated analyses of a secondary clinopyroxene standard indicate precision of ± 2% relative for major elements and ± 10% relative for minor elements.

Monazite-xenotime thermometry

Analyses of monazite and xenotime (Table DR7) were collected by wavelength-dispersive spectroscopy using an automated JEOL 6400 SEM fitted with three crystal spectrometers. Operating conditions of 20 kV accelerating voltage, 100 nA beam current and a spot size of 3–5 μm were employed. Synthetic phosphates and glasses (REE, Y, P); natural minerals, i.e. wollastonite (Si, Ca), corundum (Al), crocoite (Pb); synthetic ThO_2 and pure metals (Fe, U) were used as standards. Methodology for the analysis of REE followed that of Williams (1996). Data reduction used software from Moran Scientific.

Temperatures were calculated using the equation developed by Gratz and Heinrich (1998):

$$D_{Gd(T)} = -0.5586 + 1.591*10^{-3}*T(°C), \text{ where } D_{Gd(T)} = X_{Gd}^{monazite}/X_{Gd}^{xenotime}$$

SHRIMP U-Th–Pb ANALYSES – Jack Hills

Sample preparation

Samples of quartz-pebble conglomerate were collected from the W74 site at Eranondoo Hill (Wilde and Pidgeon, 1991) in the Jack Hills belt, Western Australia. A portion of the samples was crushed and heavy minerals were separated using heavy liquids. The concentrate was passed through a Franz magnetic separator and the non-magnetic fraction was again processed with heavy liquids to obtain a final zircon separate. Abundant zircon crystals were obtained from all samples. The zircons grains were cast into 25 mm resin mounts, with fragments of the BR266 reference zircon (Stern, 2001) and polished to expose the central sections of grains.

Data acquisition

Xenotime and monazite data acquisition followed established procedures (Foster et al., 2000; Rasmussen et al., 2001; Fletcher et al., 2004) except that Y and Nd were also monitored in the monazite analyses (Fletcher et al., 2010). In several instances, second analyses were made on (or overlapping) previous analytical sites. These provide additional $^{207}Pb/^{206}Pb$ data but no attempt was made to calibrate Pb/U or element abundances for the repeat analyses (i.e., no repeat analyses were recorded for the standards). Consequently, complete U, Th, Pb/U and Pb/Th data are not reported for these analyses. For element abundance determinations, Pb/U and Pb/Th calibration, and corrections for matrix effects and Pb/Pb fractionation, both xenotime and monazite made use of a suite of reference materials (see Fletcher et al., 2004; 2010) that were in a separate mount.

The zircon analyses followed routine analytical practise (e.g. Smith et al., 1998) except that they were conducted in conjunction with analyses of the inclusions and therefore used smaller primary beam diameters (spots) than is common for zircon. This necessitates using smaller primary ion currents than normal but because of the age of these zircons the Pb^+ secondary ion count rates were sufficient to give precise $^{207}Pb/^{206}Pb$ dates.

Data reduction

All data were processed using Squid-2 software (Ludwig, 2009). Both zircon and xenotime data were subjected to "exponential" calibrations for Pb/U, using $^{206}Pb^{+}/^{238}U^{+}$ as the primary data ratio, and indirect calibrations of Pb/Th. For monazite, the primary ratios for Pb/U and Pb/Th were $^{206}Pb^{+}/^{270}[UO2]^{+}$ and $^{208}Pb^{+}/^{264}[ThO2]^{+}$, both of which were subjected to 1-dimensional calibrations (Fletcher et al., 2010). Corrections for instrumental mass fractionation of Pb isotopes and for matrix effects in xenotime and monazite Pb/U and Pb/Th and were made subsequently, using spreadsheet templates.

Xenotime and monazite data were corrected, when necessary, for minor overlap of the primary ion beam onto adjacent zircon. For xenotime the extent of overlap was determined from $^{196}[Zr_2O]^{+}/^{194}[Y_2O]^{+}$; for monazite it was estimated from SEM images taken after the SHRIMP analyses. The ages and element abundances of the incorporated zircon was assumed to be the same as that recorded in the independent zircon analyses of the same grains.

Results

The zircon data (Table DR8) are mostly concordant (within 5%), giving direct age measurements for the grains. For the others, $^{207}Pb/^{206}Pb$ gives a minimum age. The cases with reverse discordance (negative values in Table DR8) are probably attributable to either matrix effects from the high U contents or associated radiation damage of the grains, while the cases with normal discordance almost certainty reflect "recent" loss of radiogenic Pb. All the $^{207}Pb/^{206}Pb$ ages are ≥3300 Ma, with several analyses on one Hadean grain giving a weighted mean $^{207}Pb/^{206}Pb$ age of 4240 ± 15 Ma (95% confidence limits).

In contrast, the xenotime inclusions (Table DR9; Figs. DR4, DR5) are all <2800 Ma, and possibly all <2700 Ma, given the poor precision of the two oldest dates. There are two distinct clusters in the $^{207}Pb/^{206}Pb$ dates, at ~2.68 Ga and ~0.8 Ga, but considerable scatter in $^{206}Pb/^{238}U$ within both clusters. Only one analysis (of an overgrowth) suggests mixing of xenotime from the two growth events.

The older cluster of xenotime data is internally consistent in $^{207}Pb/^{206}Pb$ (MSWD = 1.03), giving a weighted mean $^{207}Pb/^{206}Pb$ age of 2681 ± 7 Ma (95% confidence, including a component from data for the $^{207}Pb/^{206}Pb$ reference sample). The large range of discordance, for what appears to be a single generation of xenotime, is unusual. It is unlikely to be an instrumental effect, since there is nothing similar in concurrent data for standards, and there is variability within the sample data for each analytical session. It seems more likely that these xenotimes have unusual trace element contents or small inclusions that are imposing matrix effects on $^{206}Pb/^{238}U$ data.

The dispersion of the younger xenotime analyses is similar to that in the 2.68 Ga data, and we therefore accept the $^{207}Pb/^{206}Pb$ dates for the young group as a better measure of xenotime age than the corresponding $^{206}Pb/^{238}U$ dates. An electron microprobe analysis of a xenotime inclusion from this subset was obtained before SHRIMP analysis (0933.1-1; Table DR9; Fig. 1F). It has high Fe (2.3 wt% FeO), Th (2.7 wt% ThO by EMP, 4.6% Th by SHRIMP) and common Pb (2.4% of ^{206}Pb; Table DR9). The six young analyses give a weighted mean $^{207}Pb/^{206}Pb$ age of 790 ± 30 Ma.

The 2.68 Ga inclusions are slightly older than the 2.65 Ga ages previously recognised in monazite and xenotime in the matrix of quartz-pebble conglomerate at Eranondoo Hill and Eranondoo East (Rasmussen et al., 2010), whereas the ~0.8 Ga age agrees with the less precise younger age recorded in those rocks.

Only one monazite inclusion was large enough for SHRIMP analysis (Table DR10). It has a very high common Pb content (~50% in ^{206}Pb), possibly due to overlap onto Fe-oxide particles in the inclusion. The ^{207}Pb/^{206}Pb data are therefore not useful. The Pb/U data appear to be unstable, even allowing for calibration drift between the two sequential analyses. The ^{208}Pb/^{232}Th data appear to be the most stable, but cannot be taken to be as accurate as the precision suggests. Despite these reservations, the monazite is clearly not Archean, and most likely of similar age to the ~0.8 Ga xenotime.

SHRIMP U–Pb ANALYSES – additional samples

Samples

In order to provide additional background context for the Jack Hills samples, we have analysed several zircon-xenotime pairs in which the xenotime is completely isolated within zircon (in the plane exposed for analysis). These are from three localities in Western Australia and one in England, as listed in Table DR11.

Methods

The analyses and data reduction followed the same principles as described above, with the following minor variations.

All data for 9947C.11 were obtained in 1999 and the xenotime data for C65.7 and C65.8 were collected in 2003; primary data reduction for these analyses was by Squid-1. The other data were all collected in a single analytical session in 2010, using a <0.2 nA primary ion beam for the xenotime analyses and ~0.5 nA for zircon. The primary reference material for 9947C xenotime was S437, which also served as a reference for mass fractionation. In all other case the primary reference was CZ3 or MG-1 for zircon and xenotime, respectively, and Xeno-1 (z6413) was used to correct for mass fractionation.

Results

The relevant data are listed in Table DR11.

The C65 zircon data are consistent with a large unpublished data set that gives a 1.79 Ga age for zircons in this tuff bed in the Capricorn Formation. The xenotime dates are fall within a narrow range of ages for xenotime outgrowths on those zircons.

There are no existing data for the King Leopold Sandstone (Kimberley Group), but the zircon date is similar to detrital zircon ages commonly recorded in the Kimberly region and the xenotime date is consistent with the age of authigenic xenotime outgrowths (~1.7 Ga) on zircons in the Pentecost Sandstone and Warton Sandstone (McNaughton et al., 1999).

The Archaean age for detrital zircon in quartzite from Steere River (Mount Barren Group) is consistent with the ≥1.8 Ga sedimentary age of the succession (e.g. Dawson et al., 2002) and the xenotime date falls in the 1.2 – 1.7 Ga range of authigenic and metamorphic ages recorded previously (e.g. Vallini et al., 2002; Dawson et al., 2003; Rasmussen et al., 2006).

The Millstone Grit xenotime date is consistent with ~300 Ma (unpublished) results for xenotime outgrowths on zircon in this sample, and with the ~315 Ma depositional age of the rock, but clearly younger than the enclosing Archaean zircon.

REFERENCES CITED

Dawson, G.C., Krapež, B., Fletcher, I.R., McNaughton, N.J., and Rasmussen, B., 2002, Did late Palaeoproterozoic assembly of proto-Australia involve collision between the Pilbara,Yilgarn and Gawler Cratons? Geochronological evidence from the Mount Barren group in the Albany–Fraser Orogen of Western Australia: Precambrian Research, v. 118, p. 195–220.

Dawson, G.C., Krapez, B., Fletcher, I.R., McNaughton, N.J., and Rasmussen, B., 2003, 1.2 Ga thermal metamorphism in the Albany-Fraser Orogen of Western Australia: consequence of collision or regional heating by dyke swarms? Journal of the Geological Society, London, v. 160, p. 29-37.

Fletcher, I.R., McNaughton, N.J., Aleinikoff, J.A., Rasmussen, B., and Kamo, S.L., 2004, Improved calibration procedures and new standards for U–Pb and Th–Pb dating of Phanerozoic xenotime by ion microprobe: Chemical Geology, v. 209, p. 295–314.

Fletcher, I.R., McNaughton, N.J., Davis, W.J., and Rasmussen, B., 2010, Matrix effects and calibration limitations in ion probe U–Pb and Th–Pb dating of monazite: Chemical Geology, v. 270, p. 31-44.

Foster, G., Kinny, P., Vance, D., Prince, C., and Harris, N., 2000, The significance of monazite U-Th-Pb age data in metamorphic assemblages; a combined study of monazite and garnet chronometry: Earth and Planetary Science Letters, v. 181, p. 327–340.

Gratz, R., and Heinrich, W., 1998, Monazite-xenotime thermometry. III. Experimental calibration of the partitioning of gadolinium between monazite and xenotime: European Journal of Mineralogy, v. 10, p. 579-588.

Hopkins, M., Harrison, T.M., and Manning, C.E., 2008, Low heat flow inferred from >4 Gyr zircons suggests Hadean plate boundary interactions: Nature, v. 456, p. 493-496.

Ludwig, K.R., 2009, Squid 2; a user's manual. Berkeley Geochronology Center, 100p.

McNaughton, N.J., Rasmussen, B., and Fletcher, I.R., 1999, SHRIMP uranium–lead dating of diagenetic xenotime in siliciclastic sedimentary rocks: Science, v. 285, p. 78–80.

Muhling, J.R., 1990, The Narryer Gneiss Complex of the Yilgarn Block, Western Australia: a segment of Archaean lower crust uplifted during Proterozoic orogeny: Journal of Metamorphic Geology, v. 8, p. 47-64.

Rasmussen, B., Fletcher, I.R., and McNaughton, N.J., 2001, Dating low-grade metamorphic events by SHRIMP U–Pb analysis of monazite in shales: Geology, v. 29, p. 963–966.

Rasmussen, B., Fletcher, I.R., Muhling, J.R., and Wilde, S.A., 2010, In situ U-Th–Pb geochronology of monazite and xenotime from the Jack Hills belt: Implications for the age of deposition and metamorphism of Hadean zircons: Precambrian Research, v. 180, p. 26-46.

Rasmussen, B., Muhling, J.R., Fletcher, I.R., and Wingate, M.T.D., 2006, In situ SHRIMP U-Pb dating of monazite integrated with petrology and textures: Does bulk composition control whether monazite forms in low-Ca pelitic rocks during amphibolite facies metamorphism? Geochimica et Cosmochimica Acta, v. 70, p. 3040-3058.

Smith, J.B. *et al.,* 1998, The Sholl shear zone, West Pilbara; evidence for a domain boundary structure from integrated tectonostratigrpahic analyses, SHRIMP U–Pb dating and isotopic and geochemical data of granitoids: Precambrian Research, v. 88, p. 143-171.

Stacey, J.S., and Kramers, J.D., 1975, Approximation of terrestrial lead isotope evolution by a two-stage model: Earth and Planetary Science Letters, v. 26, p. 207–221.

Stern, R.A., 2001, A new isotopic and trace-element standard for the ion microprobe: preliminary thermal ionization mass spectrometry (TIMS) U–Pb and electron-microprobe data; Radiogenic Age and Isotopic Studies: Report 14, Geological Survey of Canada, Current Research 2001-F1, 11p.

Vallini, D., Rasmussen, B., Krapež, B., Fletcher, I.R., and McNaughton, N.J., 2002, Obtaining diagenetic ages from metamorphosed sedimentary rocks: U-Pb dating of unusually coarse xenotime cement in phosphatic sandstone: Geology, v. 30, p. 1083–1086.

Wilde, S.A., and Pidgeon, R.T., 1990, in Third International Archaean Symposium, Excursion Guidebook (eds Ho, S.E., Glover, J.E., Myers, J.S., and Muhling, J.R.) 82-95 (Geology Department, University Extension. Uni. of Western Australia Pub. no. 21).

Williams, C.T., 1996, in Rare Earth Minerals: Chemistry, Origin and Ore Deposits (eds Jones, A.P., Wall, F., and Williams, C.T.) 327-348 (Chapman and Hall).

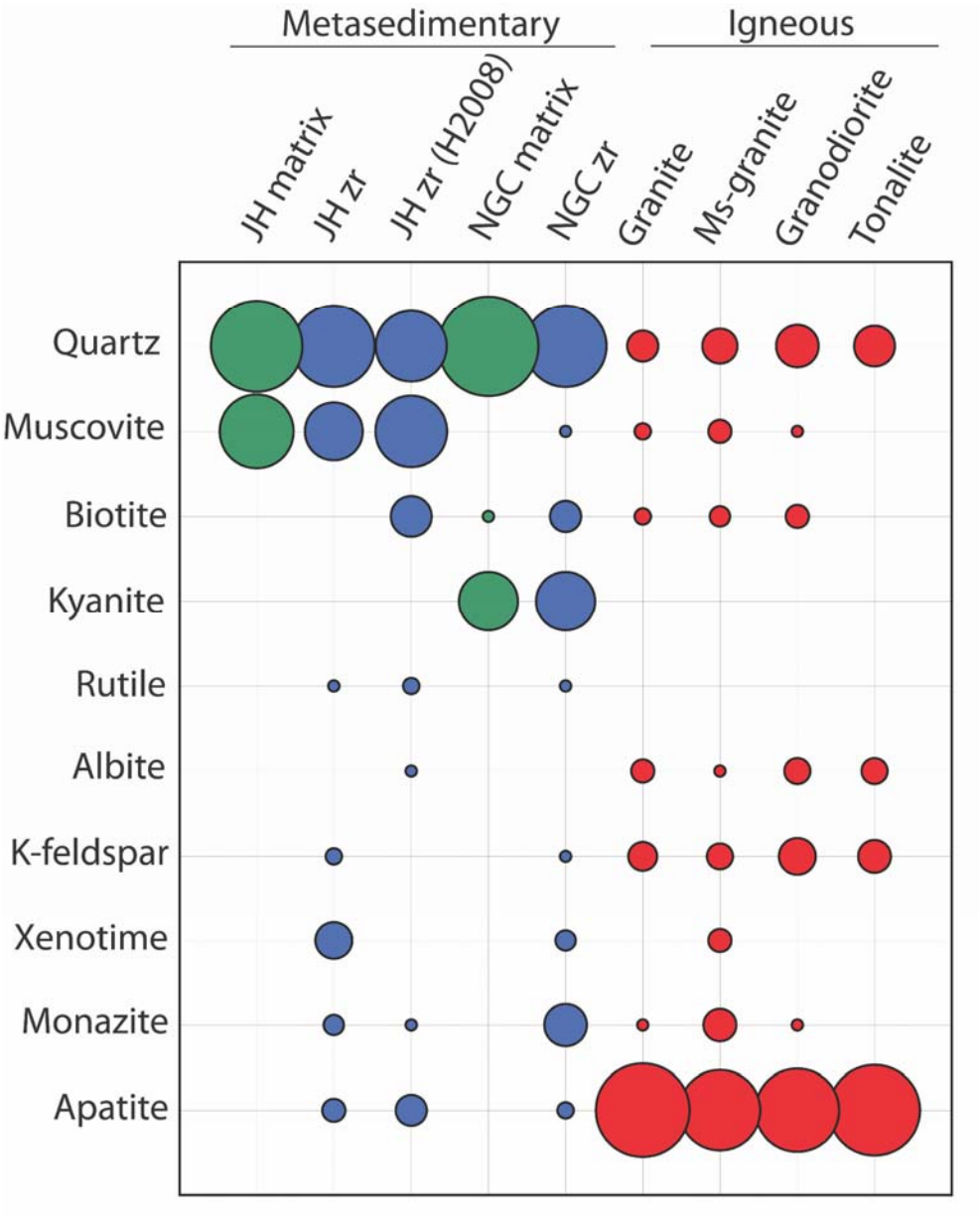

Figure DR1. Mineral inclusion data for zircon (zr) in Jack Hills (JH), the Narryer Gneiss Complex (NGC) (Table DR1) and Precambrian igneous rocks from Australia (Tables DR2 and 3). Proportions of minerals in inclusions and matrix represented by dot area. ms – muscovite. JH matrix – the metamorphic matrix of quartz-pebble conglomerate (W74); JH zr – mineral inclusions in detrital zircons from Jack Hills (W74); JH zr (H2008) – mineral inclusions in Jack Hills zircons from Hopkins et al. (2008); NGC matrix – metamorphic matrix of granulite-facies quartzites from near Errabiddy (Muhling, 1990); NGC zr – mineral inclusions in zircon from granulite-facies quartzite near Errabiddy (Muhling, 1990).

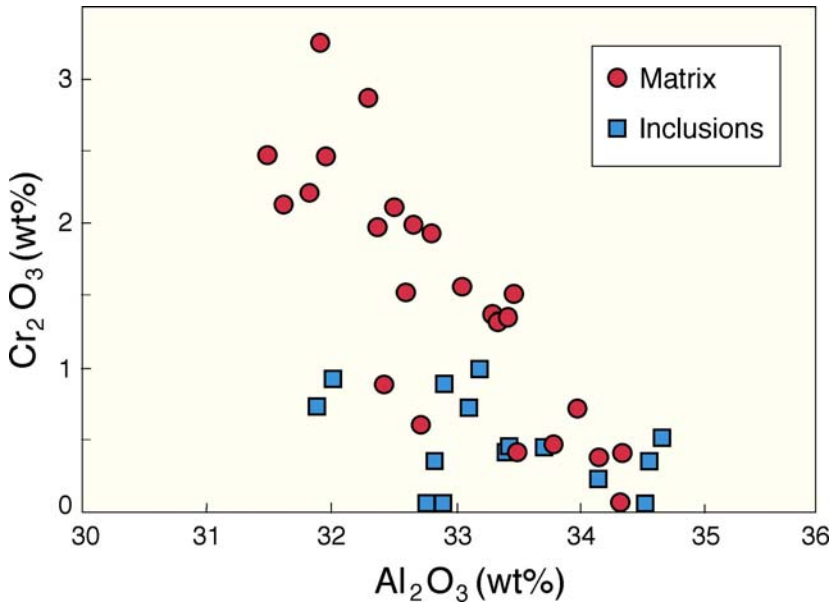

Figure DR2. Plot of Cr and Al contents in muscovite from mineral inclusions in detrital zircon grains and the metamorphic quartz-muscovite matrix. Jack Hills quartz-pebble conglomerate (W74 site).

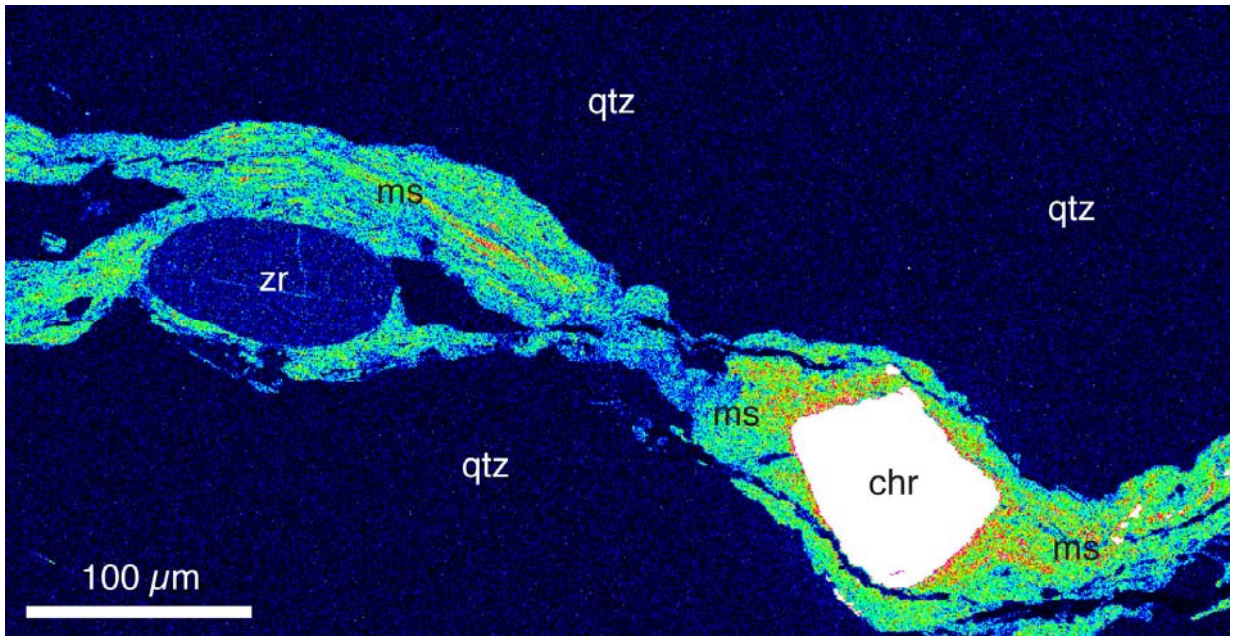

Figure DR3. Electron microprobe element map showing the concentration of Cr in the quartz-muscovite (qtz-ms) matrix. The muscovite Cr content is highly variable, with the highest values immediately adjacent to the detrital chromite grain (chr), with sharply lower Cr concentrations in muscovite around the detrital zircon grain (zr). Jack Hills quartz-pebble conglomerate (W74 site).

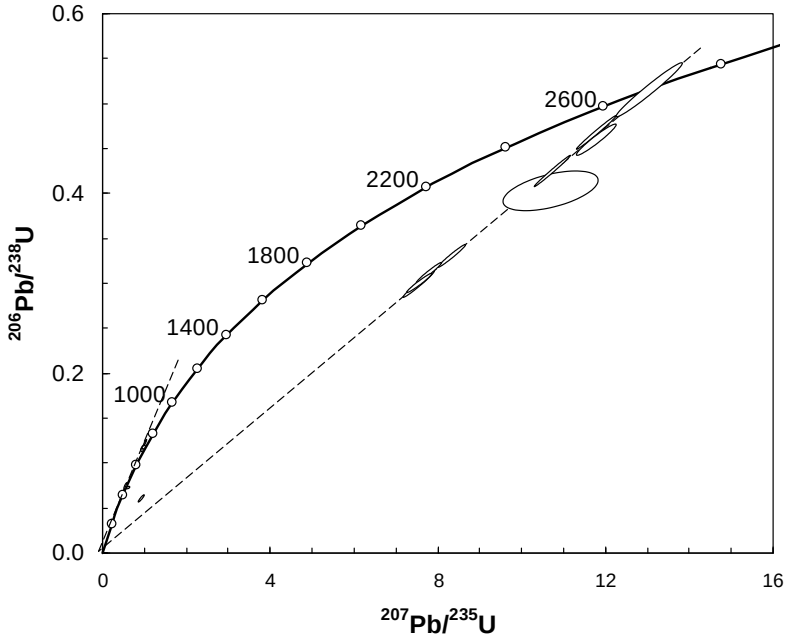

Figure DR4. U–Pb concordia plot for all analysed xenotime inclusions in Jack Hills zircons.

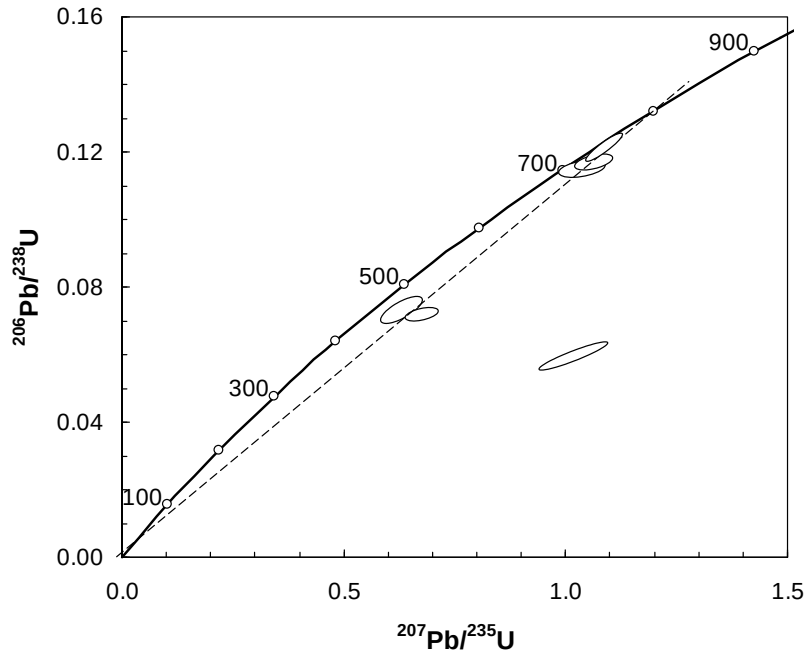

Figure DR5. U–Pb concordia plot for Neoproterozoic xenotime inclusions in Jack Hills zircons.

Table DR1**.** Mineral inclusion data for Jack Hills (JH) detrital zircons, metamorphic matrix and Precambrian igneous rocks.

Mineral Inclusion	Ms-Gr n = 3	Gr n = 13 Av (%)	GD n = 5 Av (%)	Tnl n = 4 Av (%)	NGC Qtz n = 3 Av (%)	JH zr This study Av (%)	JH zr H2008 Av (%)	JH matrix This study Av (%)
Apatite	47	63	50	59		4	7	
Monazite	8	1	1	tr	13	3	1	tr
Xenotime	4	tr			3	10		tr
K-feldspar	5	6	10	8	1	2		
Albite	1	4	5	5		tr	1	
Plagioclase		1	tr	1	tr			
Th,Si	11	2	tr	tr		tr		
U,Zr,Si-Ca		tr					1	
Muscovite	4	2	1	tr	1	24	37	39
Biotite	3	2	4	tr	7	tr	12	
Chlorite	1	4	7	1				
Quartz	9	7	13	12	48	48	36	60
Calcite	2	1	tr	1				
Epidote		3	3	4			1	
Allanite		tr	tr					
Magnetite		tr	1	1				
Fe-ox		tr		tr		8		tr
Titanite		tr	1	2				
Ti-Magnetite				1				
Ilmenite	1	tr	1	1	tr	tr	2	
Rutile				tr	1	1	2	tr
Hornblende		1	tr	tr		1		
REE-oxide				tr				
Kyanite					25			

Ms-Gr – muscovite granite; Gr – granite; GD – granodiorite; Tnl – tonalite; NGC Qtz – detrital zircon from kyanite-rich quartzite from the northern Narryer Gneiss Complex (Errabiddy), JH zr – Jack Hills detrital zircons (conglomerate from site W74); Matrix - Jack Hills matrix (conglomerate from site W74). H2008 – Hopkins et al. (2008). Tr - <0.5%.

Table DR2. Mineral inclusion data for magmatic zircon in monzogranite (MG) and syenogranite (SG).

GSWA No.	169044	178078	178049	142937	184811	169096	169097	179435	178101	178425	178103	139464	169055	169018	169062
Rock type	Ms-Bt MG	Bt MG	Bt MG	MG	Bt MG	MG	MG	Bt MG	Bt MG	Bt MG	Bt MG	MG	MG	MG	SG
Apatite	34	158	181	88	112	94	81	298	98	136	58	175	7	43	4
Monazite	1				24		1					3	22		4
Xenotime	2														1
K-feldspar	2	12	4	4	31	6	3	5	8	26	14	10	13	3	9
Albite		8	4	1	11	2	7	7	4	17	5	1	2	4	5
Plagioclase		1			1					2	4				3
Th,Si	5	56	1	2				1				1			
Th,Si,Zr	1														
U,Zr,Si-Ca					1										
Muscovite	1	2	5		8	6		2	1	6		4	10		8
Biotite	1				15			2	2	2	1	8	7		4
Chlorite		3	5	1	5	15	5	22	5	7	6	6	3	3	2
Quartz		17	23	8	12	2	11	7	14	31	9	15	26	1	9
Calcite				1	13		1	6	3	1		3	6		1
Epidote/Zoisite		40	14	1	6	1	8	21	2	9	7			2	
Allanite					1		1	5							
Magnetite		1				1									
Fe-ox								5							1
Titanite			1		1	2	1	6		1					
Ilmenite					1		2				1	1	4		
Hornblende		1			1		3	1							3
Si,Al,Fe			1												
Si,Al,Fe-Mn	1														
Al-Si					1										
ZnS								2							
PbS			1		4			8							
TOTAL	32	299	241	106	248	129	124	399	137	238	105	227	102	56	54

Table DR3. Mineral inclusion data for magmatic zircon in granodiorite (GD) and tonalite (Tnl).

GSWA No.	169028	177933	177932	178104	139466	160212	178002	178077	178102
Rock type		Hnbl		Bt		Bt-Hbl	Bt	Bt	hnbl
	GD	GD	GD	GD	GD	Tnl	Tnl	Tnl	Tnl
Apatite	660	152	103	48	27	139	116	211	130
Monazite				1	5				1
K-feldspar	71	61	7	9	10	31	18	5	29
Albite	33	24	12	9	1	19		1	39
Plagioclase					1	2	1	1	10
Th,Si		2			1	5	1		
Muscovite	8		1		2	1			
Biotite	2	2		1	15	2		1	3
Chlorite	17	42	13	20		4	5		25
Quartz	78	52	12	19	18	24	44	2	57
Calcite		4	2			4	6		
Epidote/Zoisite	9	16	11	11		7	10	2	39
Allanite		1							
Magnetite	4	5	4			2	3	2	
Fe-ox									2
Sphene		11		1		5	3	1	9
Ti-Magnetite						2		1	8
Ilmenite	4	1		2	2		2	6	
Rutile								1	
Hornblende		1	1	3				1	5
Si,Al,Fe							1		
Ce,Nd,La,Ca						1			
FeS						1			
CuS									1
Pyroxene					1				1
TOTAL	887	374	166	124	83	249	210	235	359

Table DR4. Chemical composition of muscovite in mineral inclusions from Jack Hills zircons.

Sample	jh23	jh25	jh26	jh28	jh211	jh213	jh216	jh217	jh22	jh24	jh29	jh210	brjh21	brjh24	brjh26
Oxide no.	11	11	11	11	11	11	11	11	11	11	11	11	11	11	11
SiO_2	44.92	44.98	44.41	45.09	45.43	45.52	45.30	46.25	46.87	45.69	45.45	46.99	46.25	45.99	45.73
TiO_2	0.45	0.35	b.d.	b.d.	0.25	0.38	0.13	0.35	0.32	b.d.	0.37	0.25	0.53	0.17	0.45
Al_2O_3	31.89	34.15	33.10	34.66	34.53	32.02	34.55	32.83	32.89	33.72	33.42	32.77	32.91	33.19	33.40
Cr_2O_3	0.73	0.23	0.72	0.51	b.d.	0.92	0.35	0.35	b.d.	0.45	0.45	b.d.	0.89	0.99	0.42
Fe_2O_3	b.d.	b.d.	b.d.	b.d.	b.d.	b.d.	b.d.	b.d.	b.d.	b.d.	b.d.	b.d.	b.d.	b.d.	b.d.
FeO	1.80	1.41	1.70	1.14	1.44	1.68	1.23	1.16	1.36	1.47	1.58	1.48	1.43	1.56	1.85
MnO	b.d.	0.15	b.d.	b.d.	b.d.	b.d.	b.d.	b.d.	b.d.	b.d.	b.d.	b.d.	b.d.	b.d.	b.d.
MgO	1.29	0.95	0.93	0.76	0.90	1.08	0.73	1.31	1.03	0.99	0.80	0.96	0.96	1.01	0.85
CaO	b.d.	b.d.	b.d.	b.d.	b.d.	b.d.	b.d.	b.d.	b.d.	b.d.	b.d.	b.d.	b.d.	b.d.	b.d.
Na_2O	0.58	0.69	0.69	0.81	0.58	0.57	0.69	0.65	0.57	0.44	0.69	0.46	0.50	0.67	0.55
K_2O	10.65	10.82	10.54	10.70	10.60	10.45	10.40	10.34	10.74	10.66	10.13	10.52	10.51	10.69	10.83
Cl	b.d.	b.d.	b.d.	b.d.	b.d.	b.d.	b.d.	b.d.	b.d.	b.d.	b.d.	b.d.	b.d.	b.d.	b.d.
Oxide total	**92.31**	**93.73**	**92.09**	**93.67**	**93.73**	**92.62**	**93.38**	**93.24**	**93.78**	**93.42**	**92.89**	**93.43**	**93.98**	**94.27**	**94.08**
Si	3.116	3.065	3.084	3.066	3.082	3.138	3.081	3.147	3.173	3.112	3.110	3.188	3.133	3.115	3.106
Al	0.884	0.935	0.916	0.934	0.918	0.862	0.919	0.853	0.827	0.888	0.890	0.812	0.867	0.885	0.894
Al	1.724	1.808	1.794	1.844	1.843	1.740	1.851	1.781	1.798	1.820	1.806	1.809	1.761	1.766	1.780
Ti	0.023	0.018	0.000	0.000	0.013	0.020	0.007	0.018	0.016	0.000	0.019	0.013	0.027	0.009	0.023
Cr	0.040	0.012	0.040	0.027	0.000	0.050	0.019	0.019	0.000	0.024	0.024	0.000	0.048	0.053	0.023
Fe^{3+}	0.000	0.000	0.000	0.000	0.000	0.000	0.000	0.000	0.000	0.000	0.000	0.000	0.000	0.000	0.000
Fe^{2+}	0.104	0.080	0.099	0.065	0.082	0.097	0.070	0.066	0.077	0.084	0.090	0.084	0.081	0.088	0.105
Mn	0.000	0.009	0.000	0.000	0.000	0.000	0.000	0.000	0.000	0.000	0.000	0.000	0.000	0.000	0.000
Mg	0.133	0.096	0.096	0.077	0.091	0.111	0.074	0.133	0.104	0.101	0.082	0.097	0.097	0.102	0.086
	2.024	**2.023**	**2.029**	**2.013**	**2.029**	**2.018**	**2.021**	**2.017**	**1.995**	**2.029**	**2.021**	**2.003**	**2.014**	**2.018**	**2.017**
Ca	0.000	0.000	0.000	0.000	0.000	0.000	0.000	0.000	0.000	0.000	0.000	0.000	0.000	0.000	0.000
Na	0.078	0.091	0.093	0.107	0.076	0.076	0.091	0.086	0.075	0.058	0.092	0.061	0.066	0.088	0.072
K	0.943	0.941	0.934	0.928	0.918	0.919	0.903	0.898	0.928	0.927	0.885	0.911	0.909	0.924	0.939
	1.021	**1.032**	**1.027**	**1.035**	**0.994**	**0.995**	**0.994**	**0.984**	**1.003**	**0.985**	**0.977**	**0.972**	**0.975**	**1.012**	**1.011**
Cl-	0.000	0.000	0.000	0.000	0.000	0.000	0.000	0.000	0.000	0.000	0.000	0.000	0.000	0.000	0.000
Cation total	**7.050**	**7.060**	**7.060**	**7.050**	**7.020**	**7.010**	**7.010**	**7.000**	**7.000**	**7.010**	**7.000**	**6.970**	**6.990**	**7.030**	**7.030**

Table DR5. Chemical composition of muscovite in rock matrix from quartz-pebble conglomerate.

Sample ID	chr14	chr15	chr18	chr19	ch112	ch115	ch117	chr21	chr25	chr26	chr29	ch214	ch215	ch216	chr17	ch218	ch219
Ox no	11	11	11	11	11	11	11	11	11	11	11	11	11	11	11	11	11
SiO_2	46.37	46.72	46.93	45.97	45.60	47.79	47.85	48.66	44.68	45.20	45.43	46.97	47.10	44.75	46.74	45.18	46.14
TiO_2	0.58	0.43	0.60	0.90	0.60	0.67	0.55	0.18	0.62	0.67	0.58	0.53	0.75	0.55	0.43	0.50	0.63
Al_2O_3	32.51	33.06	32.66	31.92	32.60	34.34	33.79	29.26	31.62	31.83	32.30	32.38	33.47	32.72	33.42	32.43	33.34
Cr_2O_3	2.11	1.56	1.99	3.25	1.52	0.41	0.47	1.81	2.13	2.21	2.87	1.97	1.51	0.61	1.35	0.89	1.32
Fe_2O_3	b.d.	b.d.	b.d.	b.d.	b.d.	b.d.	b.d.	b.d.	b.d.	b.d.	b.d.	b.d.	b.d.	b.d.	b.d.	b.d.	b.d.
FeO	1.66	1.59	1.44	1.50	1.56	1.31	1.56	1.31	1.79	1.50	1.58	1.66	1.56	1.58	1.50	1.48	1.39
MnO			b.d.	b.d.	b.d.	b.d.	b.d.	b.d.	b.d.	b.d.	b.d.	b.d.	b.d.	b.d.	b.d.	b.d.	b.d.
MgO			1.09	1.04	1.11	0.86	1.08	0.98	1.13	2.02	0.96	1.08	0.80	1.18	1.01	0.93	0.99
CaO			b.d.	b.d.	b.d.	b.d.	b.d.	b.d.	b.d.	b.d.	b.d.	b.d.	b.d.	b.d.	b.d.	b.d.	b.d.
Na_2O	0.46	0.53	0.44	0.59	0.57	0.58	0.66	0.28	0.69	0.59	0.55	0.66	0.71	0.44	0.66	0.47	0.53
K_2O	10.33	10.60	10.82	10.53	10.65	10.91	10.57	11.13	9.81	10.39	10.59	10.56	10.21	10.15	10.19	9.88	10.81
Cl	b.d.	b.d.	b.d.	b.d.	b.d.	b.d.	b.d.	b.d.	b.d.	b.d.	b.d.	b.d.	b.d.	b.d.	b.d.	b.d.	b.d.
Oxide total	**95.11**	**95.53**	**95.99**	**95.52**	**94.18**	**96.99**	**96.58**	**94.65**	**92.30**	**93.47**	**94.70**	**95.91**	**96.32**	**91.73**	**95.28**	**91.66**	**95.02**
Si	3.117	3.123	3.127	3.094	3.100	3.131	3.148	3.285	3.099	3.100	3.084	3.134	3.115	3.105	3.122	3.131	3.102
Al	0.883	0.877	0.873	0.906	0.900	0.869	0.852	0.715	0.901	0.900	0.916	0.866	0.885	0.895	0.878	0.869	0.898
Al	1.693	1.728	1.693	1.627	1.713	1.784	1.769	1.613	1.685	1.674	1.669	1.681	1.725	1.782	1.753	1.780	1.745
Ti	0.029	0.022	0.030	0.046	0.031	0.033	0.027	0.009	0.032	0.035	0.030	0.027	0.037	0.029	0.022	0.026	0.032
Cr	0.112	0.082	0.105	0.173	0.082	0.021	0.024	0.097	0.117	0.120	0.154	0.104	0.079	0.033	0.071	0.049	0.070
Fe^{3+}	0.000	0.000	0.000	0.000	0.000	0.000	0.000	0.000	0.000	0.000	0.000	0.000	0.000	0.000	0.000	0.000	0.000
Fe^{2+}	0.093	0.089	0.080	0.084	0.089	0.072	0.086	0.074	0.104	0.086	0.090	0.093	0.086	0.092	0.084	0.086	0.078
Mn	0.000	0.000	0.000	0.000	0.000	0.000	0.000	0.000	0.000	0.000	0.000	0.000	0.000	0.000	0.000	0.000	0.000
Mg	0.109	0.104	0.110	0.086	0.109	0.096	0.111	0.203	0.099	0.110	0.081	0.117	0.100	0.096	0.099	0.086	0.086
	2.036	**2.025**	**2.018**	**2.016**	**2.024**	**2.006**	**2.017**	**1.996**	**2.037**	**2.025**	**2.024**	**2.022**	**2.027**	**2.032**	**2.029**	**2.027**	**2.011**
Ca	0.000	0.000	0.000	0.000	0.000	0.000	0.000	0.000	0.000	0.000	0.000	0.000	0.000	0.000	0.000	0.000	0.000
Na	0.060	0.069	0.057	0.077	0.075	0.074	0.084	0.037	0.093	0.078	0.072	0.085	0.091	0.059	0.085	0.063	0.069
K	0.886	0.904	0.920	0.905	0.924	0.912	0.887	0.959	0.868	0.909	0.917	0.899	0.862	0.899	0.869	0.874	0.928
	0.946	**0.973**	**0.977**	**0.982**	**0.999**	**0.986**	**0.971**	**0.996**	**0.961**	**0.987**	**0.989**	**0.984**	**0.953**	**0.958**	**0.954**	**0.937**	**0.997**
Cl-	0.000	0.000	0.000	0.000	0.000	0.000	0.000	0.000	0.000	0.000	0.000	0.000	0.000	0.000	0.000	0.000	0.000
Cation total	**6.980**	**7.000**	**7.000**	**7.000**	**7.020**	**6.990**	**6.990**	**6.990**	**7.000**	**7.010**	**7.010**	**7.010**	**6.980**	**6.990**	**6.980**	**6.960**	**7.010**

Table DR6. Chemical composition of muscovite in rock matrix from quartz-pebble conglomerate.

Sample ID	mnxe12	mnxe13	mnxe15	ran1	ran2	ran3	ran4	ran5
Oxygen no.	11	11	11	11	11	11	11	11
SiO_2	45.35	46.39	46.54	46.52	46.20	45.24	46.76	45.62
TiO_2	0.73	0.60	0.72	0.57	0.48	0.60	0.58	0.53
Al_2O_3	31.49	31.96	33.30	34.15	33.49	32.81	34.32	33.98
Cr_2O_3	2.47	2.46	1.37	0.38	0.42	1.93	b.d.	0.72
Fe_2O_3	b.d.	b.d.	b.d.	b.d.	b.d.	b.d.	b.d.	b.d.
FeO	1.68	1.40	1.54	1.53	1.58	1.12	1.48	1.50
MnO	b.d.	b.d.	b.d.	b.d.	b.d.	b.d.	0.30	b.d.
MgO	0.83	0.86	0.88	1.04	0.75	0.91	0.93	0.73
CaO	b.d.	b.d.	b.d.	b.d.	b.d.	b.d.	b.d.	b.d.
Na_2O	0.49	0.51	0.63	0.80	0.47	0.59	0.69	0.65
K_2O	10.33	10.21	10.70	10.15	10.50	10.57	10.29	10.58
Cl	b.d.	b.d.	b.d.	b.d.	b.d.	b.d.	b.d.	b.d.
Oxide total	**93.42**	**94.57**	**95.55**	**95.01**	**94.37**	**93.59**	**95.10**	**94.39**
Si	3.114	3.134	3.112	3.108	3.119	3.090	3.117	3.082
Al	0.886	0.866	0.888	0.892	0.881	0.910	0.883	0.918
Al	1.663	1.679	1.737	1.798	1.784	1.732	1.814	1.788
Ti	0.038	0.030	0.036	0.029	0.024	0.031	0.029	0.027
Cr	0.134	0.131	0.072	0.020	0.022	0.104	0.000	0.038
Fe^{3+}	0.000	0.000	0.000	0.000	0.000	0.000	0.000	0.000
Fe^{2+}	0.096	0.079	0.086	0.085	0.089	0.064	0.083	0.085
Mn	0.000	0.000	0.000	0.000	0.017	0.000	0.000	0.000
Mg	0.090	0.105	0.075	0.091	0.094	0.074	0.097	0.082
	2.021	**2.024**	**2.006**	**2.023**	**2.030**	**2.005**	**2.023**	**2.020**
Ca	0.000	0.000	0.000	0.000	0.000	0.000	0.000	0.000
Na	0.065	0.067	0.082	0.104	0.062	0.078	0.089	0.085
K	0.905	0.880	0.913	0.866	0.905	0.921	0.875	0.912
	0.970	**0.947**	**0.995**	**0.970**	**0.967**	**0.999**	**0.964**	**0.997**
Cl-	0.000	0.000	0.000	0.000	0.000	0.000	0.000	0.000
Cation total	**6.990**	**6.970**	**7.000**	**6.990**	**7.000**	**7.010**	**6.990**	**7.020**

Table DR7. Chemical composition of monazite and xenotime from inclusions in Jack Hills zircons and rock matrix.

	inclusion-1 mon	inclusion-1 xen	inclusion-2 mon	inclusion-2 xen	matrix mon	matrix mon	matrix xen	matrix xen
SiO_2	0.68	2.09	0.28	2.06	0.38	0.17	1.41	1.26
P_2O_5	29.68	32.41	29.66	33.74	28.65	29.38	32.62	33.22
La_2O_3	12.71	0.14	14.71	0.09	17.46	15.98	0.07	0.14
Ce_2O_3	29.55	0.19	28.47	0.21	33.51	31.41	0.15	0.22
Pr_2O_3	3.54	0.13	3.19	0.04	3.31	3.56	0.19	0.11
Nd_2O_3	12.85	0.58	13.10	0.48	10.96	12.42	0.31	0.29
Sm_2O_3	2.23	1.24	3.52	1.27	1.50	1.78	1.57	1.70
Eu_2O_3	0.01	0.18	0.24	0.10	0.20	0.04	0.27	0.13
Gd_2O_3	0.54	3.88	0.61	4.26	0.35	0.38	5.85	4.74
Tb_2O_3	0.08	0.72	0.38	1.05	0.29	0.12	1.11	0.82
Dy_2O_3	0.32	4.83	0.26	5.88	0.16	0.28	7.62	6.84
Ho_2O_3	0.04	0.96	0.07	1.10	b.d.	0.02	1.21	1.26
Er_2O_3	0.08	3.61	0.17	3.45	0.04	0.14	3.77	3.87
Tm_2O_3	b.d.	0.50	0.01	0.46	b.d.	0.02	0.32	0.30
Yb_2O_3	0.04	3.79	0.06	2.40	0.09	b.d.	2.47	2.83
Lu_2O_3	b.d.	0.60	0.04	0.41	0.16	b.d.	0.37	0.34
Y_2O_3	1.41	39.02	0.45	42.11	0.49	1.24	40.65	41.64
CaO	1.24	0.22	0.82	0.10	0.62	1.17	0.11	0.16
FeO	2.89	1.81	0.27	0.28	0.67	0.39	0.58	0.79
Al_2O_3	0.20	0.24	0.13	0.27	0.13	0.01	b.d.	b.d.
PbO	0.07	0.55	0.16	0.58	0.01	0.06	0.46	0.40
ThO_2	1.21	3.06	1.51	1.63	0.26	0.33	0.10	0.14
UO_2	0.11	0.76	0.17	0.50	0.11	b.d.	0.43	0.36
TOTAL	**99.47**	**101.51**	**98.26**	**102.47**	**99.32**	**98.89**	**101.68**	**101.56**
Cation formula based on 4 oxygens								
Si	0.026	0.070	0.010	0.067	0.015	0.007	0.048	0.042
P	0.958	0.918	0.898	0.931	0.964	0.977	0.939	0.948
La	0.179	0.002	0.194	0.001	0.256	0.232	0.001	0.002
Ce	0.412	0.002	0.373	0.003	0.488	0.452	0.002	0.003
Pr	0.049	0.002	0.042	0.000	0.048	0.051	0.002	0.001
Nd	0.175	0.007	0.167	0.006	0.156	0.174	0.004	0.004
Sm	0.029	0.014	0.043	0.014	0.021	0.024	0.018	0.020
Eu	0.000	0.002	0.003	0.001	0.003	0.001	0.003	0.001

Gd	0.007	0.043	0.007	0.046	0.005	0.005	0.066	0.053
Tb	0.001	0.008	0.004	0.011	0.004	0.001	0.012	0.009
Dy	0.004	0.052	0.003	0.062	0.002	0.004	0.084	0.074
Ho	0.001	0.010	0.001	0.011	0.000	0.000	0.013	0.014
Er	0.001	0.038	0.002	0.035	0.000	0.002	0.040	0.041
Tm	0.000	0.005	0.000	0.005	0.000	0.000	0.003	0.003
Yb	0.000	0.039	0.001	0.024	0.001	0.000	0.026	0.029
Lu	0.000	0.006	0.000	0.004	0.002	0.000	0.004	0.003
Y	0.029	0.695	0.008	0.730	0.010	0.026	0.736	0.747
Ca	0.048	0.008	0.179	0.003	0.026	0.049	0.004	0.006
Fe	0.092	0.051	0.008	0.007	0.022	0.013	0.017	0.022
Al	0.009	0.010	0.005	0.010	0.006	0.000	0.000	0.000
Pb	0.001	0.005	0.002	0.005	0.000	0.001	0.004	0.004
Th	0.010	0.023	0.012	0.012	0.002	0.003	0.001	0.001
U	0.001	0.006	0.001	0.004	0.001	0.000	0.003	0.003
TOTAL	**2.032**	**2.016**	**1.963**	**1.992**	**2.032**	**2.022**	**2.030**	**2.030**
T °C	472		468				418	429

Table DR8. SHRIMP U–Pb data for Jack Hills zircons with xenotime or monazite inclusions or overgrowths, in $^{207}Pb/^{206}Pb$ sequence.

Analysis spot	U (ppm)	Th (ppm)	Th/U	f206 (%)	$^{207}Pb^*/^{206}Pb^*$	±	$^{206}Pb^*/^{238}U$	±	$^{207}Pb^*/^{235}U$	±	$^{208}Pb^*/^{232}Th$	±	Disc. (%)	$^{207}Pb^*/^{206}Pb^*$ Age (Ma)	± (Ma)
0932.1-2	521	149	0.30	0.54	0.2693	0.0046	0.389	0.009	14.46	0.41	0.086	0.005	36	3300	27
0932.2-2	61	48	0.81	1.03	0.2762	0.0059	0.616	0.028	23.45	1.16	0.145	0.011	7	3339	34
0935.3-2	273	124	0.47	-0.08	0.2767	0.0024	0.682	0.017	26.01	0.68	0.192	0.007	0	3344	14
0934.3-3	213	73	0.35	0.00	0.2779	0.0027	0.670	0.018	25.69	0.73	0.168	0.010	1	3351	15
0802.2-5	1530	1330	0.90	0.23	0.2823	0.0031	0.802	0.025	31.22	1.03	0.226	0.009	-13	3376	17
0802.2-4	921	755	0.85	0.09	0.2866	0.0063	0.755	0.028	29.85	1.30	0.183	0.009	-7	3399	34
0934.1-2	249	219	0.91	0.07	0.2839	0.0023	0.714	0.017	27.94	0.72	0.183	0.006	-3	3384	13
0802.3-2	1010	585	0.60	0.15	0.2845	0.0036	0.897	0.033	35.17	1.37	0.244	0.012	-22	3388	20
0935.4-2	111	84	0.78	0.13	0.2872	0.0031	0.697	0.018	27.59	0.77	0.181	0.006	0	3403	17
0802.1-3	1640	990	0.62	0.07	0.2874	0.0034	0.740	0.023	29.30	0.97	0.179	0.008	-5	3403	18
0935.1-2	279	165	0.61	0.00	0.3008	0.0025	0.700	0.017	29.03	0.75	0.179	0.006	2	3474	13
0935.2-2	361	140	0.40	0.05	0.3015	0.0022	0.709	0.016	29.49	0.69	0.179	0.006	1	3478	11
0934.2-2	122	80	0.68	-0.07	0.3040	0.0035	0.712	0.023	29.84	1.01	0.189	0.009	1	3491	18
0933.2-1	173	53	0.32	-0.03	0.3043	0.0028	0.672	0.015	28.18	0.67	0.172	0.005	5	3492	14
0933.1-3	281	78	0.29	0.04	0.4974	0.0034	0.878	0.016	60.24	1.18	0.185	0.006	4	4233	10
0933.1-4	287	210	0.76	0.04	0.5019	0.0043	0.878	0.016	60.74	1.22	0.205	0.006	4	4247	13
0933.1-2	83	49	0.61	0.08	0.5041	0.0063	0.914	0.064	63.51	4.51	0.214	0.017	2	4251	18

Analysis identification is nnnn.p-q where nnnn is the SHRIMP mount number, p is the zircon grain and q is the analysis site in the zircon.
Listed uncertainties are 1σ. They include all components of statistical precision.
U and Th abundances are considered accurate to ~10% and internally comparable to ~5%.
All Pb isotope data have been corrected for common Pb, using a modelled common Pb isotopic composition from Stacey and Kramers (1975) at the approximate age of the zircon. 4f206 is the apparent common Pb in ^{206}Pb, calculated from observed mass-204 counts.
Disc. is apparent U–Pb discordance, defined as $100*(1-t[^{206}Pb/^{238}U]/t[^{207}Pb/^{206}Pb])$.

Table DR9. SHRIMP U–Pb data for metamorphic xenotime associated with detrital zircons from Jack Hills.

Analysis	U (ppm)	Th (ppm)	Th/U	4f206 (%)	$^{207}Pb^*/^{206}Pb^*$	±	$^{206}Pb^*/^{238}U$	±	$^{207}Pb^*/^{235}U$	±	Disc. (%)	$^{207}Pb^*/^{206}Pb^*$ Age (Ma)	±
Archean inclusions													
0802.2-1	1220	1920	1.60	0.45	0.1929	0.0113	0.4029	0.0147	10.724	0.686	21	2767	96
0802.2-1x				1.62	0.1864	0.0039						2711	34
0802.2-2	2480	348	0.14	0.01	0.1825	0.0007	0.4690	0.0122	11.803	0.310	7	2676	6
0802.2-2x				0.87	0.1831	0.0019						2681	17
0802.3-1	5010	16400	3.30	0.08	0.1834	0.0006	0.4254	0.0114	10.800	0.290	15	2684	5
0934.1-1	5890	10000	1.70	0.58	0.1822	0.0010	0.3117	0.0075	7.898	0.195	35	2673	9
0934.3-1	4110	9950	2.40	0.07	0.1835	0.0015	0.5157	0.0199	13.324	0.517	0	2685	13
0934.3-2	4440	30800	6.90	0.55	0.1831	0.0010	0.3308	0.0084	8.387	0.218	31	2682	9
0935.1-1	5680	11800	2.10	0.49	0.1841	0.0012	0.2992	0.0096	7.648	0.250	37	2691	11
0935.2-1	2550	3100	1.20	0.33	0.1835	0.0011	0.3004	0.0072	7.617	0.187	37	2685	10
0935.2-1b				0.24	0.1822	0.0015						2673	13
0935.3-1	3100	1320	0.42	0.17	0.1858	0.0014	0.4601	0.0118	11.864	0.314	10	2705	12
0935.3-1b				0.11	0.1800	0.0015						2653	14
Neoproterozoic inclusions													
0934.2-1	3510	13700	3.90	0.03	0.0649	0.0007	0.1217	0.0028	1.089	0.027	4	771	21
0934.2-1b				0.40	0.0666	0.0011	0.1236	0.0028	1.135	0.031	9	825	34
Inclusion in contact with monazite													
0933.1-1	8660	45500	5.30	2.37	0.0687	0.0022	0.0721	0.0012	0.689	0.026	49	888	65
Outgrowths													
0802.1-1	8770	38900	4.40	1.36	0.1235	0.0023	0.0600	0.0027	1.039	0.051	81	2007	33
0802.1-2	6670	30000	4.50	1.34	0.0629	0.0021	0.0735	0.0026	0.648	0.032	35	704	70
0932.1-1	2450	4600	1.90	0.28	0.0655	0.0020	0.1152	0.0016	1.040	0.032	11	789	63
0932.2-1	3490	9460	2.70	0.05	0.0658	0.0015	0.1174	0.0016	1.066	0.027	11	801	47

Analysis identification is nnnn.p-q where nnnn is the SHRIMP mount number, p is the zircon grain and q is the analysis site for xenotime associated with that grain. Postscript b indicates a second analysis on the site; x is a revisited site. Element abundances and ratios are not independently calibrated for repeats.
Listed uncertainties are 1σ. They include all components of statistical precision and an assumed 33% uncertainty in corrections applied for zircon included in the analysed area. There are unquantified additional uncertainties in Pb/U arising from inter-mount effects and matrix effects.
U and Th abundances are considered accurate to ~25% and internally comparable to ~10%.
All Pb isotope data have been corrected for common Pb, using a modelled common Pb isotopic composition from Stacey and Kramers (1975) at the approximate age of the xenotime. 4f206 is the apparent common Pb in ^{206}Pb, calculated from observed mass-204 counts.
Disc. is apparent U–Pb discordance, defined as $100*(1-t[^{206}Pb/^{238}U]/t[^{207}Pb/^{206}Pb])$.

Table DR10. SHRIMP U–Pb data for metamorphic monazite inclusion in a detrital zircon from Jack Hills.

Analysis	U (ppm)	Th (ppm)	Th/U	4f206 (%)	$^{207}Pb^*/^{206}Pb^*$	±	$^{206}Pb^*/^{238}U$	±	Disc. (%)	4f208 (%)	$^{208}Pb^*/^{232}Th$	±	$^{208}Pb^*/^{232}U$ Age (Ma)	±
0935.1-1	56	3627	65	58	0.105	0.059	0.445	0.039	-39	38	0.0330	0.0013	656	25
0935.1-1x				46	0.199	0.042	*0.219*	*0.023*	*55*	*34*	*0.0348*	*0.0016*	*691*	*31*

Analysis identification is nnnn.p-q where nnnn is the SHRIMP mount number, p is the zircon grain and q is the analysis site for xenotime associated with that grain. Postscript x is indicates a revisited site. Element abundances and ratios are not independently calibrated for the repeat analysis, but some of the data are shown (*in italics*) to indicate the relative stability of the different data ratios.

Listed uncertainties are 1σ. They include all components of statistical precision. There are unquantified additional uncertainties of up to ~2% in Pb/U and Pb/Th arising from inter-mount effects and matrix effects.

All Pb isotope data have been corrected for common Pb, using a modelled common Pb isotopic composition from Stacey and Kramers (1975) at the approximate age of the xenotime. 4f206 (4f208) is the apparent common Pb in ^{206}Pb (^{208}Pb), calculated from observed mass-204 counts.

Disc. is apparent U–Pb discordance, defined as $100*(1-t[^{206}Pb/^{238}U]/t[^{207}Pb/^{206}Pb])$.

Table DR11. SHRIMP U–Pb data for secondary xenotime inclusions apparently isolated within zircon.

Sample	grain	Zircon age (Ma)	±	Xenotime age (Ma)	±
Capricorn Formation	C65.7	1813	18	1762	9
Capricorn Formation	C65.8	1819	15	1752	9
		1770	16		
Kimberley Group	A08.10	>1797		1692	19
Mount Barren Group	9947C.11	2637	32	1480	43
Millstone Grit	9978.15	2704	22	294	6

Grain identification is nnnn.p where nnnn is the SHRIMP mount number and p is the zircon grain number.

The ages are from $^{207}Pb/^{206}Pb$ except for the Millstone Grit xenotime, which is from $^{206}Pb/^{238}U$.

All data are concordant (within 5% or 1σ) except for zircon in the Kimberley Group, which is listed as a 1σ minimum age limit, from the measured $^{207}Pb/^{206}Pb$ date of 1815 ± 18.

Listed uncertainties are 1σ. They include internal precision, external precision (reproducibility, gauged from reference standards), 1SE uncertainty in data for reference standards, and 1% assumed systematic uncertainty in matrix corrections for xenotime Pb/U.

All data have been corrected for common Pb, using a modelled common Pb isotopic composition from Stacey and Kramers (1975) at the approximate age of the analysed sample.